

**Synthesis and Characterization of Graphene-Reinforced Polymer
Filaments for Additive Manufacturing**

by

SEAN MENEZES

Presented to the Faculty of the Graduate School of
The University of Texas at Arlington in Partial Fulfillment

Of the Requirements

For the Degree of

MASTER OF SCIENCE IN MECHANICAL ENGINEERING

THE UNIVERSITY OF TEXAS AT ARLINGTON

DECEMBER 2021

Supervising Committee:

Dr. Michael Bozlar
Dr. Ankur Jain
Dr. Erika La Plante

Copyright © by SEAN MENEZES, 2021

All Rights Reserved



Acknowledgments

December 17, 2021

I would like to thank Dr. Michael Bozlar and Dr. Ankur Jain for the assistance and guidance provided throughout my research. I would also like to thank them for helping me with my thesis and providing useful tips for developing my work. I am extremely grateful for the opportunity provided to work in the Bozlar Nanoscience Laboratory and Microscale Thermophysics Laboratory.

I would like to thank Dr. Erika La Plante for taking the time of their schedule and being a part of my thesis committee, providing me with valuable advice on my work.

I would like to thank Mr. Ashish Lal, Mr. Nitish Kallakuri, Mr. Maksim Larionov and Mr. Swapnil Salvi for the aid and the assistance they provided in the laboratory.

Lastly, I would like to thank my parents Mr. Walter and Mrs. Philomena Menezes for trusting me and supporting me in every part of my life.

Abstract

Synthesis and Characterization of Graphene-Reinforced Polymer Filaments for Additive Manufacturing

SEAN MENEZES

The University of Texas at Arlington, 2021

Supervising Professors: Michael Bozlar, Ankur Jain

Fused Deposition Modeling (FDM) is a popular 3D printing process which uses a spool of thermoplastic polymer filament that is melted by the movable extruder printer head onto the bed to generate the required shape. The most used polymer filaments in FDM are Acrylonitrile Butadiene Styrene (ABS) and Poly Lactic Acid (PLA). However, these conventional polymer filaments have lower mechanical strength and are more susceptible to cracking as the cooler parts of the printed part shrink so much that they cause cracks to develop, leading to warping. The current investigation focuses on the synthesis of graphene, synthesis of polymer filaments and characterization techniques for further development of graphene reinforced polymer filaments. Graphene is made from a single layer of carbon atoms arranged in a hexagonal lattice. The improved thermal transport properties provided by graphene to the polymer will lead to a lower heat differential between layers being printed and prevent warping from occurring. The high strength to weight ratio of graphene will lead to the formation of mechanically stronger 3D printed parts. The synthesis of graphene carried out in the lab led to the development of successful batches of functionalized graphene that can be used in the development of graphene reinforced polymer filaments. With the Determination of the relationship of parameters between the extruder and the

winding unit, spools of uniform diameter filaments can be developed for usage. The characterization techniques developed over the course of this study prove to be accurate for the measurement of tensile strength and thermal conductivity of polymer filaments. These characterization techniques can be used for the evaluation of tensile strength and thermal conductivity of graphene-reinforced polymer filaments to show the changes developed by the introduction of graphene.

List of Illustrations

Figure 1. Schematic Diagram of an FDM process.....	3
Figure 2. Anet A8 3D Printer.....	3
Figure 3. Monomers of ABS.....	4
Figure 4. PLA Monomer.....	5
Figure 5. Mechanism of Warping.....	6
Figure 6. Layer separation.....	7
Figure 7. (a) Pristine Graphene (b) Graphene Oxide.....	9
Figure 8. Functionalized graphene structure.....	9
Figure 9.(a) Raman Optothermal measurement technique.....	11
Figure 10. Graphene oxide suspension.....	12
Figure 11. Graphene oxide concentration measurement.....	13
Figure 12. MC 5 Twin Screw Micro-Compounder.....	15
Figure 13. Fiber Winding unit.....	16
Figure 14. Pebax Pellets.....	17
Figure 15. ULTEM pellets.....	17
Figure 16. Filament spools generated.....	19
Figure 17. Diameter of filament vs winding speed.....	19
Figure 18. (a) Experiment setup (b) Schematic of the experimental layout.....	23
Figure 19. (a) Experiment setup.....	24
Figure 20. Design Fixture with Pebax filament on the left and Acetal on the right.....	25
Figure 21. $\log(\theta/\theta_b)$ vs x graphs for test filament (Pebax) and standard filament (Acetal).....	25
Figure 22. Stress strain curve for PEI ULTEM filament.....	26

Table of Contents

Acknowledgments	iii
Abstract	iv
List of Illustrations	vi
Chapter 1 Introduction	1
1.1 Fused Deposition Modeling	2
1.2 Conventional Polymer Filaments	4
1.3 Drawbacks of Conventional Polymer Filaments.....	5
Chapter 2 Graphene and the Synthesis of Graphene	8
2.1 Graphene	8
2.2 Proposed benefits of Graphene	10
2.3 Synthesis of Graphene.....	11
Chapter 3 Synthesis of Polymer Filaments.....	14
3.1 Extruder and Fiber Winder Line Setup	14
3.1.1 Extruder	14
3.1.2 Fiber Winding Unit.....	15
3.1.3 Polymers used.....	16
3.2 Determination of relation of Extrusion parameters.....	18
Chapter 4 Characterization of Polymer Filaments.....	20
4.1 Thermal conductivity measurements	20
4.1.1 Theoretical background	21
4.1.2 Experimental Setup.....	22
4.1.3 Determination of Thermal conductivity	23
4.2 Mechanical Property Measurements	26
Chapter 5 Conclusion and Future work	27
References.....	28

Chapter 1

Introduction

Fused Deposition Modeling is one of the most widely used 3D printing processes for development of parts [1]. Fused Deposition modeling provides a variety of material options for part creation [2]. The low cost of these machines makes them highly viable for the industry [2]. A large area of research is focused on the development of better material polymer filaments for improved properties in parts being printed. Conventional polymer filaments show limitations with respect to their mechanical and thermal properties. To address this issue, nanocomposite polymer filament development is taken into consideration. Since the exfoliation and characterization of monolayers of graphene in 2004, it has been referred to as a wonder material due to its exceptional mechanical and thermal properties [3]. Research is focused on the accurate dispersion of graphene in the polymer matrix. A slight addition of graphene leads to an improvement in the properties of the polymer composites. Synthesis of graphene is carried out first to develop functionalized graphene. The nanoparticles created will be dispersed in the polymer melt carried out via extrusion. The polymer melt will be extruded to develop polymer filaments of required diameter using the fiber winding unit. Characterization techniques are proposed to accurately determine the thermal properties and mechanical properties of these filaments.

1.1 Fused Deposition Modeling

Extrusion based additive manufacturing is the most popular process on the market. Fused deposition modeling (FDM) is an extrusion-based technology that uses a heated chamber to liquify polymer that is pushed out through the nozzle [2]. In FDM, heat is used to melt material through a small portable chamber. Material is fed into the heated chamber as a continuous polymer filament or in the form of pellets or powder [2]. The extrusion method works on the principle that whatever material is fed into the chamber will become a liquid which is pushed out through the die of the nozzle [2]. Pressure is applied across the chamber with the help of a tractor wheel arrangement to push the molten material out of the die. The material in the chamber should be kept in a molten state at as low a temperature as possible as some polymers undergo thermal degradation at higher temperatures[2] . Figure (1) shows the schematic diagram of an FDM process. The diameter of the nozzle controls the road width, shape and size of the filament that is extruded. The nozzle also determines the minimum feature size that can be successfully created. Any feature that is smaller than the nozzle diameter cannot be printed. FDM machines range from low-cost, small-scale machines to large scale, more variable machines [2]. Material is eventually printed out layer by layer following a predefined path in a controlled form. Figure (2) shows a typical FDM 3D printer setup.

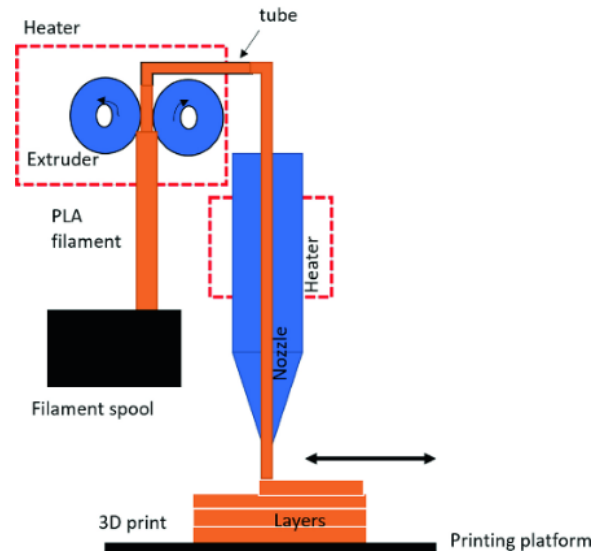


Figure 1. Schematic Diagram of an FDM process [4]

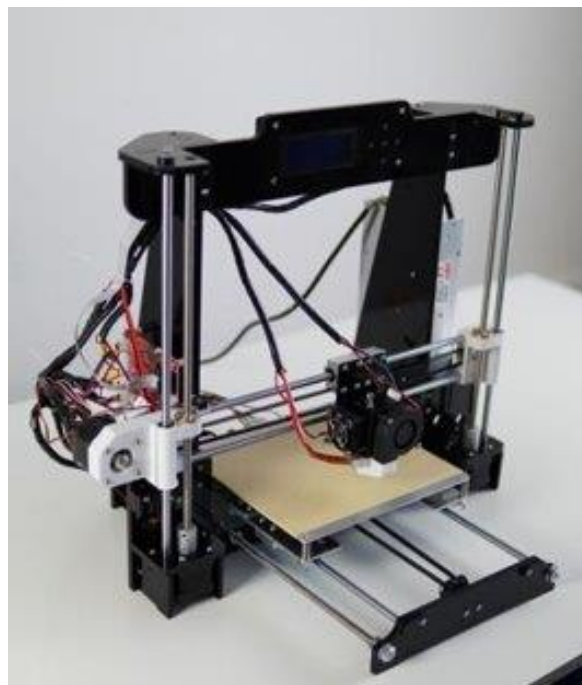


Figure 2. Anet A8 3D Printer [5]

1.2 Conventional Polymer Filaments

FDM uses polymers that are amorphous in nature as compared to polymers that show a crystalline behavior. This is because polymers require to be extruded out in a viscous paste rather than in a low viscosity form [2]. With amorphous polymers, there is no distinct melting point present, the material softens as the temperature increases. The viscosity at which these polymers are extruded out is sufficient for it to retain its shape after extrusion [2]. Solidification takes place quickly maintaining the extrusion shape. As material is added as a new layer, the previously extruded layer can easily bond with it [2].

The most widely used polymer filaments are as follows:

1. Acrylonitrile Butadiene Styrene (ABS) – Is an amorphous thermoplastic made by polymerizing styrene and acrylonitrile in the presence of butadiene. Long chains of polybutadiene are cis-crossed with shorter chains of polystyrene-co-acrylonitrile. Figure (3) shows the monomers involved in the reaction to create ABS.

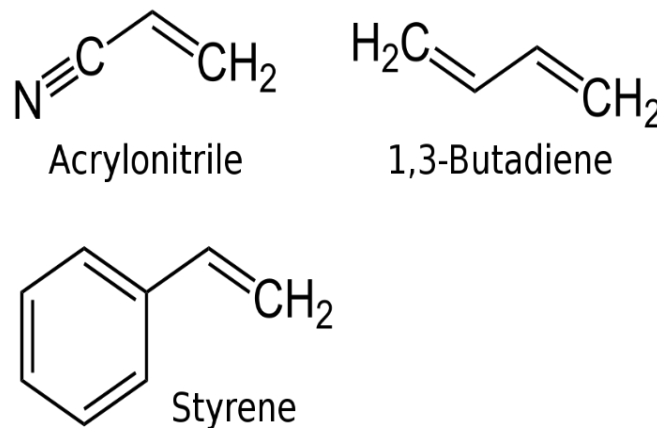


Figure 3. Monomers of ABS [6]

2. Polylactic Acid (PLA) – Is an amorphous thermoplastic polyester created by the condensation of lactic acid through renewable resources. PLA is generated from plant starch like corn or sugarcane roots. It is the default filament of choice for most FDM 3D printers[7]. Figure (4) shows the polylactic acid structure.

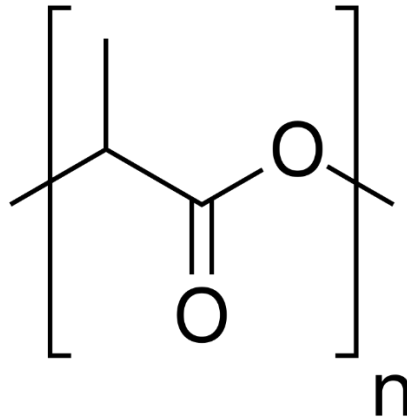


Figure 4. PLA Monomer [8]

1.3 Drawbacks of Conventional Polymer Filaments

These conventional polymer filaments are susceptible to a variety of problems that has hindered the progress of its use in major engineering applications.

The main drawbacks are as follows:

1. Susceptible to warping – As the material is being extruded in a molten form, shrinkage takes place in plastics during cooling [9]. Plastics when extruded, undergo a slight expansion which is followed by contraction after cooling down. Uneven cooling across the part leads to curling and distortion taking place. The corners of the part lift up and detach from the bed. The first few layers of the part successfully adhere to the bed, however after a few layers, due to shrinkage of the earlier

layers taking place, the part begins to curl or warp [9]. Figure (5) shows the mechanism of warping described. This warping can be so severe that it causes the part to be separated from the bed. ABS printed parts are known to shrink by almost 1.5 to 2%. For large parts, this shrinkage equals to a few millimeters of the part shrinking.

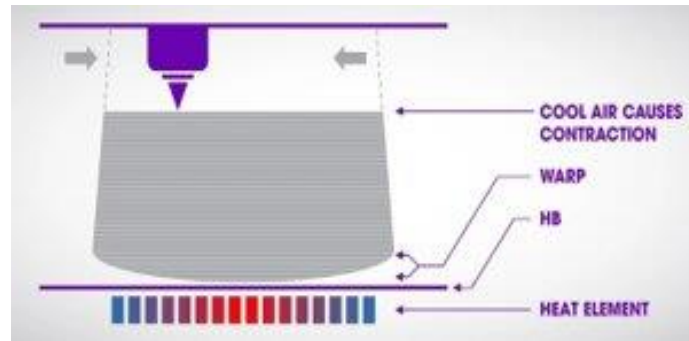


Figure 5. Mechanism of Warping [10]

2. Susceptible to layer separation – Uneven cooling across the part during extrusion leads to inadequate adhesion between subsequent layers. Layer separation takes place when a crack takes place within the part because of the forces exerted on the part, due to a different rate of cooling between layers of the 3D printed part [11]. These forces exceed the layer adhesion strength thus leading to separation between layers [11]. The mechanical strength of such parts will show a lower mechanical strength along the height of the printed part. Figure (6) is a typical example of a part where layer separation has taken place.

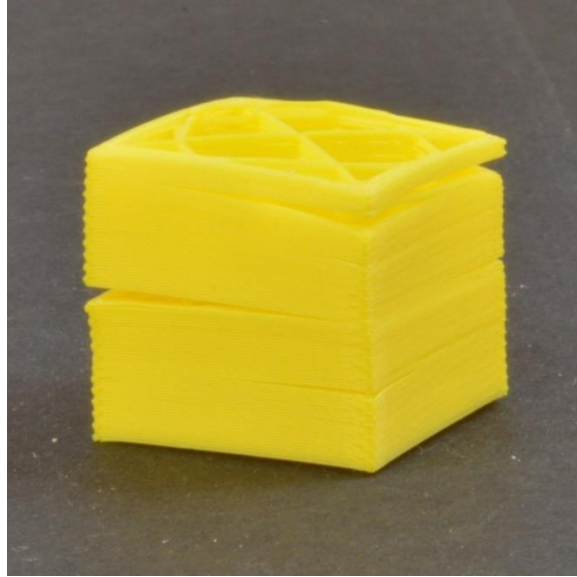


Figure 6. Layer separation [11]

Chapter 2

Graphene and the Synthesis of Graphene

2.1 Graphene

To tackle the problems being encountered from the use of conventional polymer filaments, nanoparticle-reinforced polymer filaments are being worked on. Graphene consists of single layers of carbon atoms closely packed into a two-dimensional honeycomb lattice structure. A single atomic plane is a two-dimensional structure [12]. Graphite, carbon nanotubes and fullerenes are derived from graphene. Reports on single sheets of the initial approach to the preparation of graphene took place via the micro mechanical cleavage of bulk graphite [12]. This process led to high quality pure unoxidized 2D crystals which is termed as pristine graphene; However, this process suffers from low productivity [13]. The main obstacle to obtaining individual or few-layers of graphene are the van der Waals forces between layers [13]. The route that provides graphene sheets in relative quantities is by chemical means via the oxidation of graphite. This leads to the formation of functionalized graphene. Functionalized graphene is the presence of functional groups along with graphene. The most common method to exfoliation of graphite is the use of oxidizing agents to generate graphene oxide (GO). Graphene oxide is a non-conductive hydrophilic carbon material. Various developments have taken place in the development and synthesis of graphene oxide. Brodie first carried out the synthesis of GO in 1859 with the addition of a portion of potassium chlorate to a slurry of graphite in nitric acid [13]. Staudenmaier decided to improve the synthesis carried out by Brodie with the addition of concentrated sulfuric acid, nitric acid and a few aliquots or drops of chlorate over the course of the reaction [13]. This minute change in the procedure led to highly oxidized GO being formed. In 1958, Hummer created a method which is most widely used today [13]. Graphite is oxidized by the treatment of KMnO_4 , NaNO_3 in

concentrated H_2SO_4 . All the above-mentioned methods lead to release of toxic gases during the reaction [13].

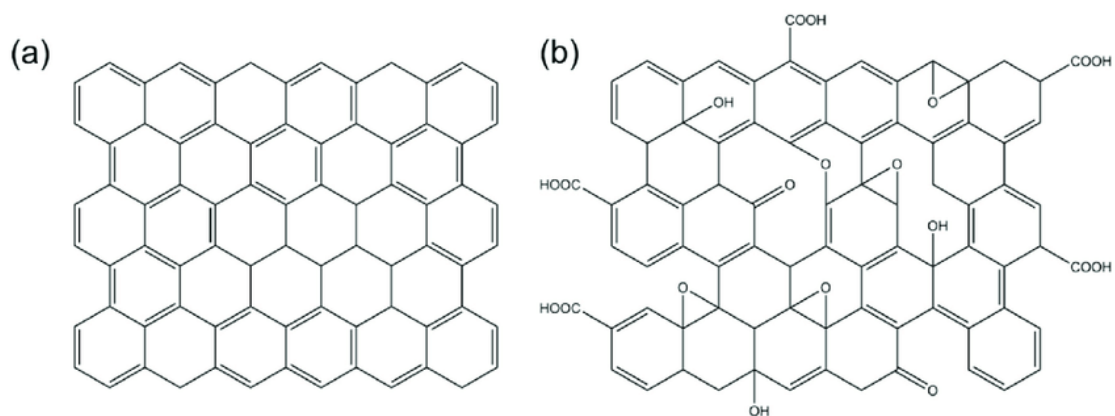


Figure 7. (a) Pristine Graphene (b) Graphene Oxide [14]

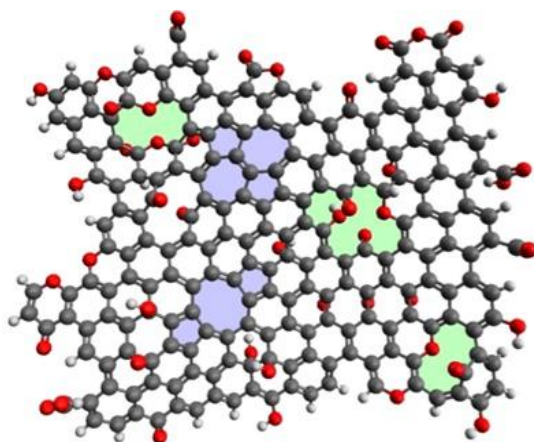


Figure 8. Functionalized graphene structure

2.2 Proposed benefits of Graphene

Due to its excellent heat conduction and mechanical properties, graphene is used to reinforce polymers to generate nanocomposite filaments.

1. Mechanical Properties – It has been shown that defect free monolayer sheets of graphene possess exceptional mechanical properties such as the modulus of elasticity of ~ 1 TPa, a strength of ~ 130 GPa[15]. This has led to the research and development of graphene reinforced polymer composites. The nanoscale surface roughness results with an enhanced interlocking with polymer chains. Graphene reinforced polymer printed parts will lead to an improved strength to weight ratio as compared to conventional polymer printed parts which correlates to improved mechanical properties.

2. Thermal Properties – Initial thermal experimental studies were carried out by University of California, Riverside. Optothermal Raman measurements were carried out on large area suspended graphene layers. The heating power was provided with the help of a laser light focused on a graphene layer connected to heat sinks at its end[16]. The temperature rise was measured with the help of a micro-Raman spectrometer [16]. Figure (9) shows the experimental setup for the initial experiments conducted to measure the thermal conductivity. The thermal conductivity was found out to be exceeding ~ 3000 W/m-K near room temperature. Following independent studies used Raman measurements along with the addition of a power meter under the suspended portion of graphene [16]. The thermal conductivity of high-quality graphene exceeded ~ 2500 W/m-K at 76 °C. The optothermal studies carried out on suspended graphene found thermal conductivity to be in the range ~ 1500 to ~ 5000 W/m-K [16]. These experimented values of graphene suggest that graphene possesses excellent thermal transport characteristics which means that uneven cooling can be controlled to obtain better layer to layer adhesion and generate a reduction in warping.

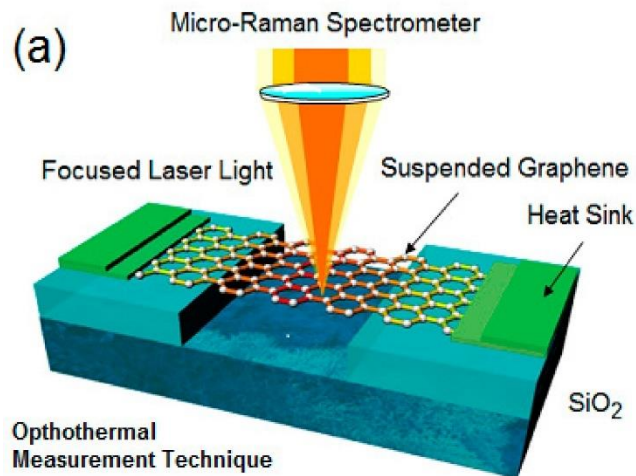


Figure 9.(a) Raman Optothermal measurement technique [16]

2.3 Synthesis of Graphene

Synthesis of Graphene via Modified Hummers method with a few changes to the entire process to optimize the GO produced was carried out at the laboratory. Any modification or variation carried out to the original Hummers method is termed as modified Hummers method [13]. The procedure carried out is a confidential procedure and hence cannot be discussed in detail. Commercially available graphene nanoplatelets were not used by us as the degree of oxidation carried out would not be as optimized as the synthesis developed. Higher degree of oxidization suggests that the presence of more functional groups prove to be better for chemistry and generate better compatibility as compared to pristine graphene. This provides a convenient method to the implementation of solution-phase techniques for the conversion of graphene oxide to graphene via chemical reduction [17]. Dispersion of graphene oxide in organic solvents is desirable as it

facilitates the practical use of the material [17]. The extent of improvement in the properties of the composite depends on the degree of dispersion of functionalized graphene in the polymer matrix.

The synthesis took place with Modified Hummer's method. After the crucial chemical reaction, washing of the graphene oxide suspension was carried out. Figure (10) shows the graphene oxide suspension prior to washing. This process is a fairly time intensive process and had to be carried out with extreme care. Improper washes result in inefficient removal of unwanted chemicals and by-products from the reaction volume. After successive washes are carried out, the final GO suspension is then validated by measuring the concentration of GO in the slurry generated. The slurry requires to be liquid enough so that a proper flow takes place for accurate measurement.

Initial centrifuge washes with an older centrifuge led to inefficient washes taking place. These inefficient washes led to the suspension being too acidic. Validation of the concentration of GO in the mixture was not possible. Eventually, the centrifuge washes were carried with a newer centrifuge. Each wash was carried out at 4500 rpm for an hour. This resulted in efficient washes taking place, the concentration of GO was then measured. Figure (11) shows the GO concentration measurement being carried out with the petri dish heated at 45 °C.

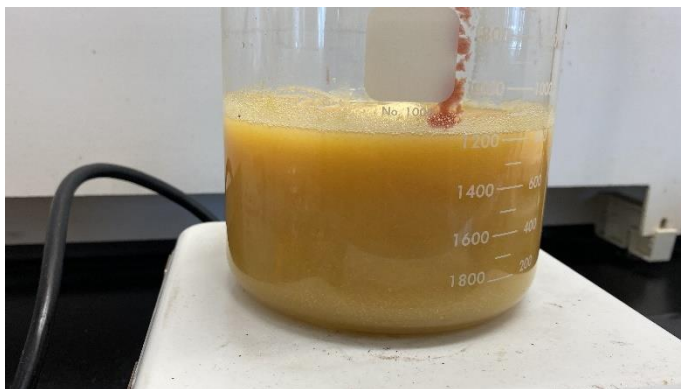


Figure 10. Graphene oxide suspension



Figure 11. Graphene oxide concentration measurement

Chapter 3

Synthesis of Polymer Filaments

Synthesis of polymer filaments were carried out in the laboratory using an extruder and a fiber winding unit. Polymer pellets were fed into the extruder, the polymer melt was extruded out in the form of filaments. The filaments were then attached to the fiber winding unit to develop control over the diameter of the filament.

3.1 Extruder and Fiber Winder Line Setup

3.1.1 Extruder

The extruder is a vertical twin screw micro compounder made by Xplore instruments. The capacity of the extruder is 5 cm³. Material is fed into the extruder in the form of polymer pellets using a hopper. The extruder provides control over the temperature and the screw speeds required to achieve successful extrusion. Three separate heating zones are present along the barrel of the extruder offer very good control over the processing temperature. Twin screws provide more torque input which allows for homogenous mixing to take place within the extruder. Excellent mixing reduces the processing time [18]. The extruder has two dies of dimensions 0.5 mm and 2 mm diameters respectively. The polymer melt comes out in the form of filaments. Polymers with a melting point of up to 400 °C can be extruded out. The extruder is provided with an air cooling and a water-cooling bracket to provide the cooling necessary once extrusion has taken place. Figure (12) shows the MC 5 extruder used to carry out extrusions in the laboratory.



Figure 12. MC 5 Twin Screw Micro-Compounder

3.1.2 Fiber Winding Unit

The winding unit is designed to collect small amounts of filament like material in combination with an extrusion unit. The winding unit is used to stretch and elongate the filament like material that is generated. The fiber line allows you to obtain long continuous fibers from just 5 to 10 grams of material input in the extruder. The Winding unit consists of a godet roll and an uptake roll. The unit consists of a speed regulated godet roll and an uptake roll [19]. The speed is eventually used to control the diameter of the filament. Air cooling is provided for the unit for proper functioning. Figure (13) shows the fiber winding unit present in the laboratory.



Figure 13. Fiber Winding unit

3.1.3 Polymers used

Synthesis of filaments were carried out with three polymers present in the laboratory.

The polymers used for extrusion are as follows:

1. Polyether Block amide (Pebax) – Obtained from Arkema under the brand name Pebax is a thermoplastic elastomer. It is a block copolymer obtained from the polycondensation of a carboxylic acid polyamide with an alcohol termination polyether. The polymer is made up of rigid polyamide blocks with soft polyether blocks [20]. The grade being used in the laboratory is 1074 SA 01, which consists of hydrophilic polyether. The melting point of the polymer is specified as 158 °C and extrusions are carried out at 165 to 170 °C. Figure (14) shows pellets of this grade
2. Polyetherimide (PEI) – Obtained from SABIC under the brand name Ultem is a clear, amorphous high-performance polymer [21]. The glass transition temperature of this polymer is

217 °C [21]. The extrusions are carried out at 370 to 380 °C. Figure shows (15) pellets of this grade.



Figure 14. Pebax Pellets



Figure 15. ULTEM pellets

3.2 Determination of relation of Extrusion parameters

For a successful extrusion to be carried out, the diameter of the filament being extruded out requires to be uniform across the entire length of the filament and be determined according to specifications demanded. To determine the diameter of the filament, experiments were carried out to understand the relation between the winding unit speed parameters with respect to the diameter of the filament. The screw speed was kept constant through all the extrusions carried out. A 0.5 mm diameter die was used for the extrusions carried out. Due to the diameter of the filament being lower than 0.5 mm, the dimensions were determined in microns. Different winding unit speeds were decided upon. Extrusions were carried out at 5 different winding unit speeds. 5 winding unit speeds were decided as 3, 5, 7, 9, 12 and 15 m/min to generate 5 datasets for generating a relationship.

From the set of experiments carried out, as shown in figure (17), a downward linear trend was generated which showed that with increasing winding unit speeds, the diameter of the filament reduced. The diameter of the filament at each meter was measured of the spool of filaments generated in the uptake filament rolls. A large deviation was noticed at extrusions carried out each winding unit speed. From experimental observations, by neglecting the initial and last 20 meters of the filament reduced the deviation observed. The deviation at the start takes place since the polymer filament cools unevenly, the filament must be drawn manually and brought to the godet roll before the winding unit carries the experiment out at a uniform winding unit speed. The last 20 meters of the filament shows a deviation because the flow of material out of the extruder reduces and a change in screw speed is required to carry out the material extrusion with the same winding unit parameters. Figure (16) shows the filament spools generated from the extrusions carried out.

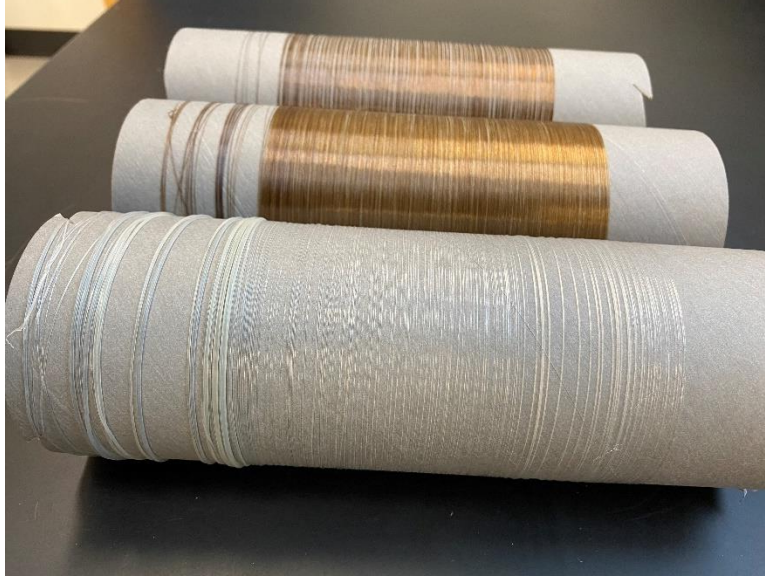


Figure 16. Filament spools generated

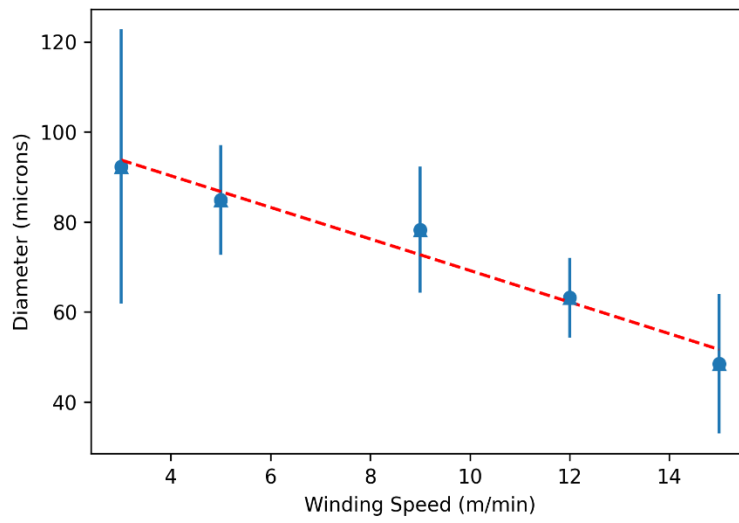


Figure 17. Diameter of filament vs winding speed

Chapter 4

Characterization of Polymer Filaments

The polymer filaments synthesized are characterized by measuring their mechanical and thermal properties. Thermal conductivity of the polymer filaments is measured using the setup developed at the Microscale thermophysics laboratory. The method allows an accurate measurement of thermal conductivity of millimeter sized wires to take place. The mechanical properties are measured using a standard test to measure the properties of a fiber from American Society of Testing and Materials (ASTM). These measurements are carried out to develop an understanding of the behavior of polymer filaments.

4.1 Thermal conductivity measurements

Thermal conductivity is defined as the rate at which heat passes through a specific material. It is the measure of a material's ability to conduct heat [22]. It is characterized by Fourier's law. Fourier's law relates the heat flux with the temperature rise. A variety of measurement techniques are available to determine the thermal conductivity of a material. Most measurement techniques rely on the application of a steady state heat flux to a sample and find the thermal response of the sample [22]. The experimentally determined value is validated with the help of an analytical model of heat transfer that takes place. However, most of these measurement techniques are not suitable for the measurement of filaments or wires that are a few mm in diameter [23]. Primary reasons being the fact that heat loss takes place across the filament's perimeter, and it is very difficult to establish a steady state heat flux through the cross section of the filament [23]. The measurement technique developed at the laboratory focuses on an infrared thermography-based measurement of the temperature distribution across the cross-section of the wires suspended from a block kept at

high temperature [23]. A comparison is carried out between the filament whose thermal response needs to be found and a filament whose thermal conductivity is already known.

4.1.1 Theoretical background

Consider a long cylindrical filament of length L and diameter D . The length of the filament is long enough for it to be considered as an infinite fin . The thermal conductivity of the filament requires to be measured [23]. The filament is attached to one end of a large body that is kept at a base temperature T_b . The temperature of the environment is measured as T_a . The filament loses heat from its periphery to the surrounding environment. The aspect ratio of the filament is assumed to be very large to keep the thermal conduction in the filament one-dimensional. The Radial Biot number is less than 0.1, therefore the thermal gradient across the radial direction is negligible. Temperature rise is kept small enough for linear radiative heat transfer coefficient to be developed. From all these assumptions, by using the fin-equation [24], the temperature distribution can be determined as follows:

$$\frac{d^2\theta}{dx^2} - \frac{hP}{kA_c}\theta = 0 \quad (1)$$

Where $\theta = T(x) - T_a$ i.e., the temperature rise compared to the environment. $P = \pi D$ is the perimeter and $A_c = \frac{\pi D^2}{4}$ is the cross-sectional area of the filament. h is the heat transfer coefficient for radiation and convection. It is assumed to be independent of temperature.

The boundary conditions for Eq (1) are as follows:

$$\theta(x=0) = \theta_b \quad (2)$$

$$\text{as } x \rightarrow \infty, \theta \rightarrow 0 \quad (3)$$

Therefore, the temperature distribution within the fin can be derived as [24]

$$\frac{\theta}{\theta_b} = e^{-mx} \quad (4)$$

From Eq (4), m can be determined by finding the slop of the plot $\log (\theta/\theta_b)$ versus length (x). If the filament geometry and the convective heat transfer coefficient is known, the thermal conductivity can be determined. As the convective heat transfer coefficient of the filament is very difficult to determine, a comparative analysis is carried out. A filament of known thermal conductivity called the standard filament S and the test filament T whose thermal conductivity is required to be determined are considered. As both filaments are subjected to the same conditions, a ratio can be developed to determine the parameter m.

$$\frac{m_S}{m_T} = \sqrt{\frac{k_T D_T}{k_S D_S}} \quad (5)$$

If the diameters are similar and the ambient conditions remain the same, Equation (5) can assume that the heat transfer coefficient for both filaments is the same [23]. This equation can be further simplified to

$$k_T = k_S \frac{D_S m_S^2}{D_T m_T^2} \quad (6)$$

The above equation shows that the thermal conductivity of the test filament can be determined by knowing the values of m^2 and the thermal conductivity of the standard filament [23].

4.1.2 Experimental Setup

The two filaments are suspended on an Aluminum block with a design fixture used to keep the filaments in a horizontal fashion. The filaments and the design fixture are coated with graphite spray for a uniform emissivity to be present across the filaments. A thin coating of graphite is required on the filaments. Thermal interface material is applied between the Instec heater, the aluminum block, and the filaments to ensure that minimal interfacial temperature drop takes place

[23]. The heater is an Instec HCS662V thermal stage that is kept at a constant temperature. FLIR A6703sc infrared camera is used to generate the thermal images of the filaments. The infrared camera is placed on a specific setup design to measure the temperature and not be disturbed during the temperature measurement [23]. Based on the length of the filament, the positioning stage can be moved to cover the entire length of the filament. Figure (18) shows the picture of the setup and the schematic layout of the experiment.

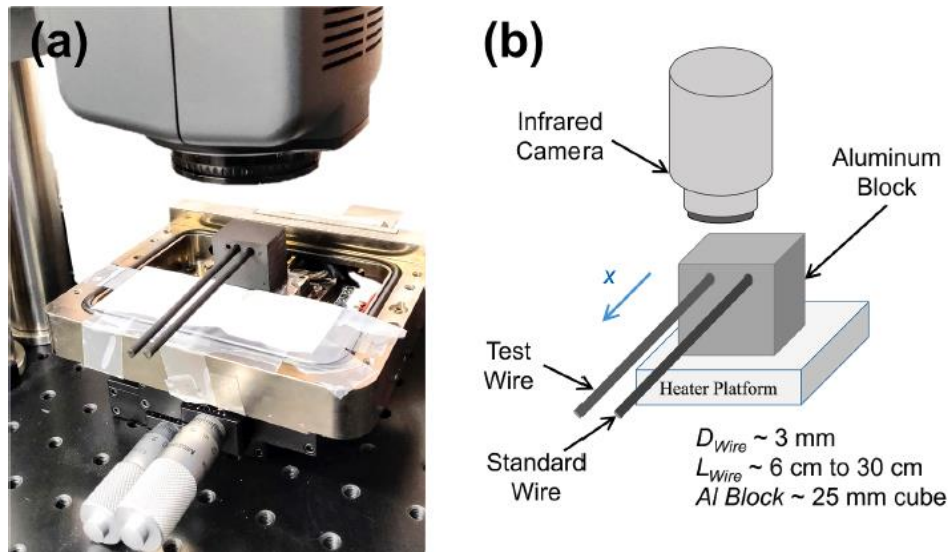


Figure 18. (a) Experiment setup (b) Schematic of the experimental layout [22]

4.1.3 Determination of Thermal conductivity

Experiments were carried out to determine the thermal conductivity of polyether block amide (pebax) filaments. Acetal filament was decided as the standard filament with the known thermal conductivity being $k_s = 0.23 \text{ W/m-K}$. Figure (19) shows the experimental setup for the measurement to be carried out. The experiment cannot be carried out with filaments of diameters

lower than 2 mm, as the temperature drop for thinner filaments is a lot more, which leads to a larger m value. The m value affects the thermal conductivity value found, due to this the diameters of the filaments were $D_S = 3.20$ mm and $D_T = 2.74$ mm. Figure (20) shows the polymer filaments placed on the block parallel to each other. The Instec thermal stage was set at 35 °C. The filaments were placed parallel to each other with a gap of at least 3.0 mm to prevent thermal cross talk from taking place. The ambient temperature was measured as $T_a = 22.5$ °C. Figure (21) shows the plot generated for the two filaments in the experiment. The $\log(\theta/\theta_b)$ vs x graph were generated with R^2 value greater than 0.85 for both cases. A linear trend can be noticed for both polymer filaments. Thermographs of the final length and at the tip of the filaments were not taken into consideration as thermal decay is exponential. As the temperature of the filament goes closer to the ambient temperature, the temperature rise near the tip of the filament will be small and will affect the thermal conductivity measurement.

Thermal conductivity of the test filament was found out to be 0.2588 W/m-K. As the exact value of thermal conductivity of Pebax filaments are unknown, the value was verified with the thermal conductivity of an epoxy polymer which is around 0.17 W/m-K.



Figure 19. (a) Experiment setup



Figure 20. Design Fixture with Pebax filament on the left and Acetal on the right

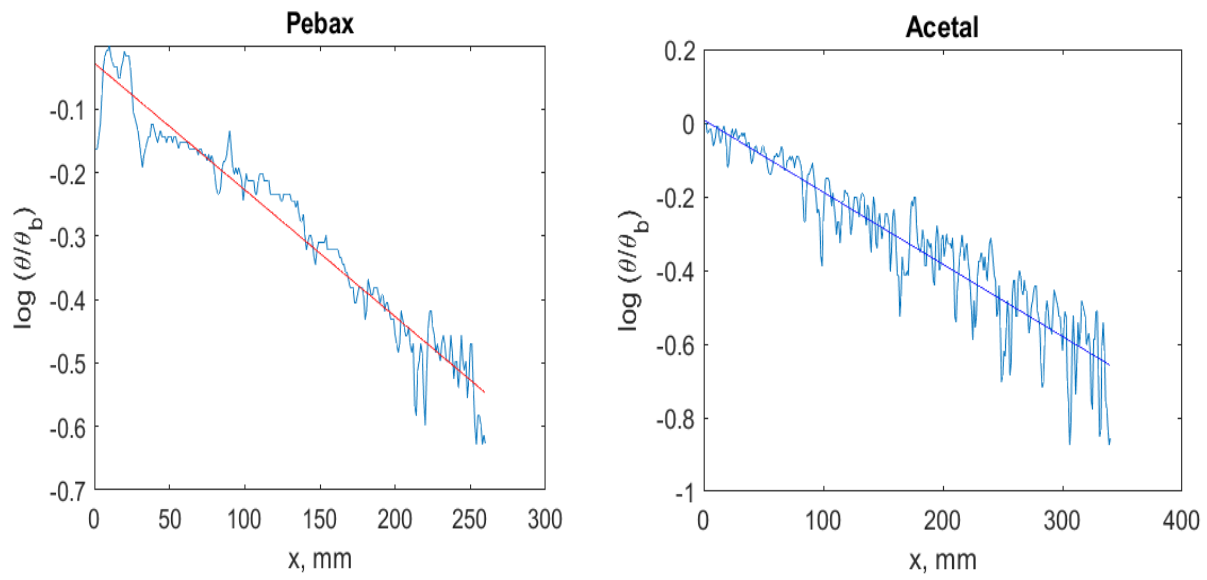


Figure 21. $\log(\theta/\theta_b)$ vs x graphs for test filament (Pebax) and standard filament (Acetal)

4.2 Mechanical Property Measurements

Determination of the tensile strength of the polymer filament is crucial for the understanding of the behavior of the filament under various loading conditions. Initial measurements of mechanical properties were carried out using ASTM's standard test method for measuring the tensile strength of fibers. The measurement is carried out ambient temperature. The fiber is mounted in the testing machine where it is subjected to a constant displacement [25]. A test result is valid if the failure does not take place in the gripping region of the fiber. The stress strain curve is generated from the experiment carried out [25]. The experiments were carried out on polyetherimide filaments. Fig shows the stress strain curve from mechanical testing of polyetherimide filaments.

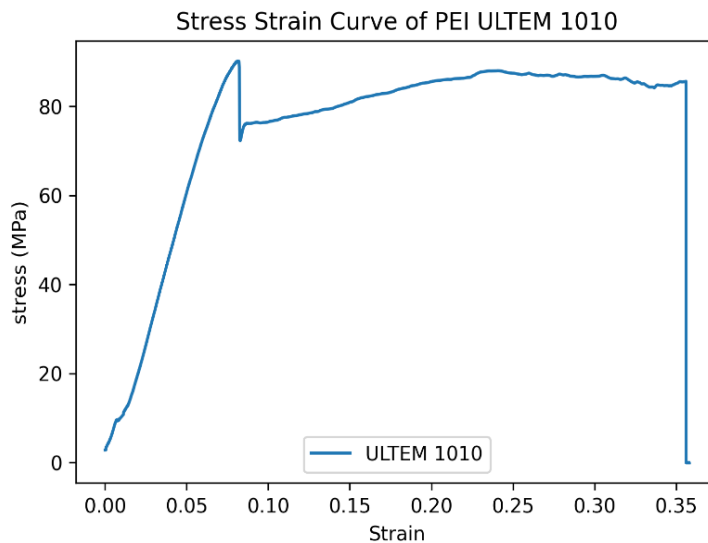


Figure 22. Stress strain curve for PEI ULTEM filament

Chapter 5

Conclusion and Future work

The graphene synthesized in the laboratory show a high degree of oxidization which provides a better dispersion of graphene in the polymer matrix. These batches of graphene developed in the lab can be used for successful development of graphene reinforced polymer filaments with homogenous dispersion of graphene within the filaments.

Determination of the relationship of parameters during extrusion of polymer filaments shows that the diameter of the polymer filaments generated can be closely controlled to develop polymer filaments with uniform diameter across the entire length of the filament spool developed. Twin screws present in the extruder provide homogenous mixing which suggests that a more homogenous polymer melt can be developed which is crucial for the introduction of graphene in the polymer melt.

The characterization techniques carried out in this thesis prove to be effective and accurate for the measurement of crucial properties of the polymer filaments that are synthesized. The thermal conductivity measurement is efficient with low and high thermal conductivity materials; thus, they can be used to accurately measure the thermal conductivity and tensile strength of nanocomposite polymer filaments.

Future work includes , the graphene synthesized in the laboratory will be compounded with polymer pellets to develop graphene reinforced polymer nanocomposite filaments. The characterization techniques developed will be used to measure the change in thermal conductivity and tensile strength of graphene reinforced polymer filaments as compared to these filaments without any nanoparticles. These nanocomposite filaments will be used as a filament spool to 3D

print a standard part with the Anet A8 3D printer present in Microscale Thermophysics Laboratory. A dog bone sample will be 3D printed to carry out mechanical property testing of the 3D printed part to develop an understanding on the change in mechanical properties via the introduction of graphene. Fox 50 instrument is an instrument used to measure the thermal conductivity of materials ranging from 0.1 to 10 W/m-K. For an accurate measurement to take place, the sample needs to be of specific dimensions. A rectangular block of two thicknesses will be 3D printed using the nanocomposite filament spool and used to find the thermal conductivity with the Fox 50 instrument.

References

- [1] Gao, X., Yu, N., & Li, J. (2020). Influence of printing parameters and filament quality on structure and properties of polymer composite components used in the fields of automotive. In K. Friedrich, R. Walter, C. Soutis, S. G. Advani, & I. H. B. Fiedler (Eds.), *Structure and Properties of Additive Manufactured Polymer Components* (pp. 303–330). Opgehaal van <https://www.sciencedirect.com/science/article/pii/B9780128195352000107>
- [2] Gibson, Rosen, D. W., & Stucker, B. (2010). *Additive manufacturing technologies : rapid prototyping to direct digital manufacturing* . Springer.
- [3] Shafraniuk. (2015). *Graphene : fundamentals, devices, and applications* . CRC Press. <https://doi.org/10.1201/b18258>
- [4] Khan. (2021). A comprehensive review on effect of printing parameters on mechanical properties of FDM printed parts. *Materials Today: Proceedings*. <https://doi.org/10.1016/j.matpr.2021.09.433>
- [5] <https://all3dp.com/1/anet-a8-3d-printer-review-diy-kit/> (12/15/2021)
- [6] https://upload.wikimedia.org/wikipedia/commons/0/05/ABS_Monomers_V3.svg (12/17/2021)
- [7] <https://www.simplify3d.com/support/materials-guide/pla/#:~:text=Polylactic%20Acid%2C%20commonly%20known%20as,not%20require%20a%20heated%20bed> (12/17/2021)

- [8] https://upload.wikimedia.org/wikipedia/commons/f/fa/Polylactid_skeletal.svg (12/19/2021)
- [9] <https://www.simplify3d.com/support/print-quality-troubleshooting/warping/> (12/19/2021)
- [10] <https://rigid.ink/blogs/news/3d-prints-warping-why-it-happens-and-how-to-prevent-it> (12/18/2021)
- [11] <https://www.simplify3d.com/support/print-quality-troubleshooting/layer-separation-and-splitting/> (12/18/2021)
- [12] Geim, A. K., & Novoselov, K. S. (2007). The rise of graphene. *Nature Materials*, 6(3), 183-91. doi:<http://dx.doi.org/10.1038/nmat1849>
- [13] Marcano, D. C., Kosynkin, D. V., Berlin, J. M., Sinitskii, A., Sun, Z., Slesarev, A., ... Tour, J. M. (2010). Improved Synthesis of Graphene Oxide. *ACS Nano*, 4(8), 4806–4814. doi:10.1021/nn1006368
- [14] <https://www.simplify3d.com/support/print-quality-troubleshooting/layer-separation-and-splitting/> (12/19/2021)
- [15] Rao, & Sood, A. K. (2013). Graphene synthesis, properties, and phenomena . Wiley-VCH.
- [16] Balandin, A. A. (2011). Thermal properties of graphene and nanostructured carbon materials. *Nature Materials*, 10(8), 569-81. doi:<http://dx.doi.org/10.1038/nmat3064>
- [17] Paredes, J. I., Villar-Rodil, S., Martínez-Alonso, A., & Tascón, J. M. D. (2008). Graphene Oxide Dispersions in Organic Solvents. *Langmuir*, 24(19), 10560–10564. doi:10.1021/la801744a
- [18] <https://www.xplore-together.com/products/micro-compounders-mc-5#:~:text=Micro%20compounder%205%20ml%3A%20MC%205&text=This%20micro%20compounder%20has%20a,to%20the%205%20ml%20insert.> (12/18/2021)
- [19] <https://www.xplore-together.com/products/micro-fibre-line> (12/18/2021)
- [20] <https://www.extremematerials-arkema.com/en/product-families/pebax/pebax-elastomer-material-database/products/datasheet/Pebax%20AE%20MV%201074%20SA%2001> (12/19/2021)
- [21] <https://www.sabic.com/en/products/specialties/ultem-resins/ultem-resin> (12/19/2021)
- [22] Tritt. (2004). Thermal conductivity : theory, properties, and applications . Kluwer Academic/Plenum Publishers.
- [23] Salvi, S. S., & Jain, A. (2020). Measurement of thermal conductivity of millimeter-sized wires using the fin effect. *Applied Thermal Engineering*, 178, 115482. doi:10.1016/j.applthermaleng.2020.115482
- [24] Incropera. (2007). Fundamentals of heat and mass transfer. (6th ed. / Frank P. Incropera ... [et al.]). John Wiley.
- [25] <https://www.astm.org/Standards/C1557> (12/18/2021)